Aerosol Science and Technology

ISSN: 0278-6826 (Print) 1521-7388 (Online) Journal homepage: http://www.tandfonline.com/loi/uast20

Development and field evaluation of an online monitor for near-continuous measurement of iron, manganese, and chromium in coarse airborne particulate matter (PM)

Mohammad Hossein Sowlat, Dongbin Wang, Giulia Simonetti, Martin M. Shafer, James J. Schauer & Constantinos Sioutas

To cite this article: Mohammad Hossein Sowlat, Dongbin Wang, Giulia Simonetti, Martin M. Shafer, James J. Schauer & Constantinos Sioutas (2016): Development and field evaluation of an online monitor for near-continuous measurement of iron, manganese, and chromium in coarse airborne particulate matter (PM), Aerosol Science and Technology, DOI: 10.1080/02786826.2016.1221051

To link to this article: http://dx.doi.org/10.1080/02786826.2016.1221051

Accepted author version posted online: 05 Aug 2016.
Published online: 05 Aug 2016.

AEROSOL SCIENCE AND TECHNOLOGY
http://dx.doi.org/10.1080/02786826.2016.1221051

Development and field evaluation of an online monitor for near-continuous measurement of iron, manganese, and chromium in coarse airborne particulate matter (PM)

Mohammad Hossein Sowlat[a], Dongbin Wang[a], Giulia Simonetti[a,b], Martin M. Shafer[c,d], James J. Schauer[c,d], and Constantinos Sioutas[a]

[a]Department of Civil and Environmental Engineering, University of Southern California, Los Angeles, California, USA; [b]Department of Chemistry, Sapienza University of Rome, Rome, Italy; [c]Environmental Chemistry and Technology Program, University of Wisconsin–Madison, Madison, Wisconsin, USA; [d]Wisconsin State Laboratory of Hygiene, University of Wisconsin–Madison, Madison, Wisconsin, USA

ABSTRACT

A novel air sampling monitor was developed for near-continuous (i.e., 2-h time resolution) measurement of iron (Fe), manganese (Mn), and chromium (Cr) concentrations in ambient coarse particulate matter (PM) (i.e., $PM_{10-2.5}$). The developed monitor consists of two modules: (1) the coarse PM collection module, utilizing two virtual impactors (VIs) connected to a modified BioSampler to collect ambient coarse PM into aqueous slurry samples; (2) the metal concentration measurement module, which quantifies the light absorption of colored complexes formed through the reactions between the soluble and solubilized target metals and pertinent analytical reagents in the collected slurries using a micro volume flow cell (MVFC) coupled with UV/VIS spectrophotometry. The developed monitor was deployed in the field for continuous ambient PM collection and measurements from January to April 2016 to evaluate its performance and reliability. Overall, the developed monitor could achieve accurate and reliable measurements of the trace metals Fe, Mn, and Cr over long sampling periods, based on the agreement between the metal concentrations measured via this online monitor and off-line parallel measurements obtained using filter samplers. Based on our results, it can be concluded that the developed monitor is a promising technology for near-continuous measurements of metal concentrations in ambient coarse PM. Moreover, this monitor can be readily configured to measure the speciation (i.e., water-soluble portion as well as specific oxidation states) of these metal species. These unique abilities are essential tools in investigations of sources and atmospheric processes influencing the concentrations of these redox-active metals in coarse PM.

ARTICLE HISTORY
Received 1 June 2016
Accepted 30 July 2016

EDITOR
Paul Ziemann

1. Introduction

The current body of epidemiological studies provides unequivocal evidence for the association between exposure to particulate matter (PM) and increased risk of cardiovascular, neurological as well as respiratory diseases, hospitalization, and premature death (Pope et al. 2002, 2004; Brunekreef and Forsberg 2005; Delfino et al. 2005; Dockery and Stone 2007; Perez et al. 2008; Delfino et al. 2010; Davis et al. 2013; Gauderman et al. 2015). It should be noted that most of these studies have linked the health end-points with PM mass concentrations of airborne PM; however, there is growing evidence highlighting the important role of the chemical composition of ambient PM, rather than simply the mass in driving the health outcomes (Claiborn et al. 2002; Verma et al. 2009).

Redox-active transition metals, including iron (Fe), manganese (Mn), and chromium (Cr), are among the few chemical components of ambient PM that studies have documented an association with human health impacts, likely due to their ability to induce oxidative stress (e.g., via the generation of reactive oxygen species [ROS]), which usually occurs as a cascade of events that significantly increases the ROS concentration in the target cells and causes inflammatory responses in cells and tissues (Donaldson et al. 2003; Tao et al. 2003; Delfino et al. 2005; Peters et al. 2006; Li et al. 2009). Therefore, a focus of many recent studies has been on the evaluation of sources, transport, and chemical speciation of these redox-active trace metals (Putaud et al. 2004; Moreno et al. 2006; Pérez et al. 2008; Viana et al. 2008; Putaud et al. 2010; Harrison et al. 2012; Sowlat et al. 2012, 2013; Fang et al. 2015; Hassanvand et al. 2015; Argyropoulos et al. 2016). Several studies have also examined the particle-size dependency of oxidative

CONTACT Constantinos Sioutas sioutas@usc.edu Department of Civil and Environmental Engineering, University of Southern California, 3620 S. Vermont Ave. KAP210, Los Angeles, CA 90089, USA.

potential and relationship to chemical composition (Tao et al. 2003; Valavanidis et al. 2005; Ntziachristos et al. 2007; Ayres et al. 2008; Miljevic et al. 2010; Shafer et al. 2010; Charrier and Anastasio 2012).

Nonetheless, the impact of individual chemical components of PM on the health end-points is still relatively poorly understood; therefore, the development of innovative PM measurement techniques capable of providing high-resolution of chemically speciated data and their use in concurrent toxicological studies can drastically improve our current understanding of the main PM species driving these health effects (Karlsson et al. 1997; Weber et al. 2001; Wang et al. 2015). These novel techniques will also help improve our understanding of the dynamics of atmospheric PM emission, dispersion, and fate through the provision of data with higher time resolution. In particular, the development of techniques/methods capable of measuring different forms of redox-active metals (i.e., different oxidation states as well as solubility characteristics) would be very important in studying aerosol toxicity. This is because the toxicity of PM-bound metals is significantly impacted by their solubility, with the water-soluble fraction of the redox-active metals better reflecting in many cases the bioavailable pool (Shi et al. 2003; Heal et al. 2005). In addition, in most cases, the toxicity of these metals, *per se*, is dependent upon their oxidation state (Khlystov and Ma 2006; Majestic et al. 2006, 2007).

Recently, a novel online monitor was developed and successfully applied for the near-continuous measurement of $PM_{2.5}$-associated Fe, Mn, and Cr (Wang et al. 2016). The system comprised of two modules: (1) the PM collection module employing an aerosol-into-liquid collector; and (2) the chemical analysis module employing micro volume flow cell (MVFC) coupled with spectrophotometry. One of the critical advantages of the developed system over previously available technologies (e.g., aerosol time-of-flight mass spectrometry (ATOFMS) or X-ray-fluorescence (XRF) based technologies) is that it can measure these metals in both total or water-soluble forms, as well as in different oxidation states with a relatively high time resolution (i.e., 2 h), which can provide crucial information on the biological pathways underlying the adverse health effects, which are mostly speciation-driven (Wang et al. 2016).

There has been a variety of novel technologies developed to measure the on-line concentrations metals in the fine PM size fraction, including the particle-into-liquid sampler (PILS) (Weber et al. 2001); the Cooper Xact^{TM} 625 Monitoring System; the AMMS-100 Focused Photonics, Inc. (Hangzhou, China); and the semi-continuous elements in aerosol system (SEAS) (Kidwell and Ondov 2001, 2004). Despite the recent development of these high time-resolution measurement methods for $PM_{2.5}$-bound elements, to the best of our knowledge, similar systems have not yet been developed for the measurement of redox-active metals in the coarse PM fraction ($PM_{10-2.5}$, i.e., particles with an aerodynamic diameter of between 2.5 μm and 10 μm) and, therefore, are highly needed. One of the factors hindering the development of such systems for coarse PM is the low solubility of these species in the coarse size range (Birmili et al. 2006; Wang et al. 2013), which limits the ability to accurately measure the total PM-bound concentration of the target metals. A large fraction of many of these metals and trace elements is partitioned in the coarse PM fraction (Allen et al. 2001), which further highlights the need for developing techniques capable of measuring coarse PM-bound redox-active metals with a high time-resolution. Such tools will be crucial in investigations of the health impacts induced by the coarse fraction of PM, as recent studies have indicated significant association between these metals and the redox activity of coarse PM (Becker and Soukup 2003; Becker et al. 2005; Shafer et al. 2010; Cheung et al. 2011, 2012; Wang et al. 2015). To address these needs, in the present study, we developed a new technique for near-continuous (i.e., a time resolution of 2 h) measurement of three coarse PM-bound redox-active metals, namely Fe, Mn, and Cr. Following laboratory characterization, the system was operated in the field from January to April 2016 to assess its performance and reliability with minimum supervision over a relatively long period of time. In addition, in order to check the validity of the results, the online-measured data were compared with those obtained by means of inductively coupled plasma mass spectrometry (ICP-MS) analysis conducted on filter samples collecting concurrently coarse PM through a parallel sampling system. Finally, in this article, we present the results of four months of system deployment in the field, enabling us to explore the diurnal concentration profiles of these redox-active metals in ambient coarse PM.

2. Materials and methods

2.1. Reagents and standards

The water used for the collection of ambient coarse PM and system rinsing was produced by a Millipore A-10 water purification system (EMD Millipore, Billerica, MA, USA). All the acids were trace metal grade (VWR). All the chemicals and reagents were prepared in polypropylene laboratory equipment, which were acid-washed (with either 4 M hydrochloric acid (HCl) or 4 M nitric acid (HNO_3) and water-rinsed before use. For Fe, a 1000 ppm stock solution was first prepared

gravimetrically from $(NH_4)_2Fe(SO_4)_2$ (ACS) salt, and then diluted to obtained standard solutions in the range of 0–200 ppm. The Fe analytical reagent (i.e., Ferrozine) was prepared by addition of 133 mg of ferrozine (Sigma) to 50 mL of water that contained 65 μL of 4 M HCl (Rastogi et al. 2009). The Fe reducing agent (HA) was prepared by dissolving 19.3 mg of hydroxylamine hydrochloride (HA) solid (Sigma), with a purity of 99.9999%, in 50 mL of water (Majestic et al. 2006). One molar sodium hydroxide (NaOH) solution was prepared from reagent grade NaOH solid (AMRESCO) and was used for pH adjustment.

For Mn, a 100 ppm stock solution was first prepared gravimetrically from $MnCl_2$ (ACS) salt, and then diluted to obtained standard solutions in the range of 0–100 ppm. The manganese analytical reagent (formaldoxime; FAD) was prepared by dissolving 20 g of HA in 450 ml of water, followed by the addition of 10 ml of 37% formaldehyde solution, and the solution was then made up to 500 ml with water. As with Fe, 1 M NaOH solution was used for pH adjustment. Both the Fe and Mn stock solutions were acidified to pHs below 1 using a 4 M HCl solution.

For Cr, a 100 ppm stock solution was first prepared gravimetrically from K_2CrO_7 (ACS) salt, and then diluted to obtained standard solutions in the range of 0–100 ppb. In the case of Cr, the stock solution was acidified using 4 M HNO_3. In addition, in order to prepare the chromium analytical reagent (i.e., diphenylcarbazide, DPC), 167 mg of the reagent was dissolved into 100 ml of acetone. Afterwards, it was mixed with 1.67% H_2SO_4 solution at 1:1 volume ratio (Khlystov and Ma 2006). Finally, 0.143 ml of H_2O_2 was diluted to 100 mL of 0.1 M NaOH solution to prepare the 0.1% H_2O_2 solution.

2.2. System configuration

The system configuration is presented in Figure 1. The developed system comprises two modules: (1) the coarse PM collection module, and (2) the metal concentration measurement module. The coarse PM collection module utilizes two virtual impactors (VIs) connected in parallel, coupled with a modified BioSampler (i.e., liquid impinger) (BioSampler, SKC West, Inc., Fullerton, CA, USA) technology, for which extensive details can be found elsewhere (Wang et al. 2015). Briefly, the air is drawn into two round nozzle VIs, each having a major flow rate of 100 L/min and a minor flow rate of 5 L/min. This total flow rate corresponds to a theoretical 50% cut-point of 1.5 μm in aerodynamic diameter, concentrating airborne coarse PM into the VI's minor flow. As discussed in our earlier studies (Wang et al. 2015), although the theoretical cut point of the VIs is slightly lower than the traditional definition of the coarse PM size range (i.e., 2.5 μm), this cut point was selected to ensure that the entire size range of ambient coarse PM is concentrated by the maximum enrichment factor of about 20. The two minor flows are combined into a total flow rate of 10 L/min entering the modified BioSampler, in which particles are captured in 20 mL of ultrapure water to form a particle-liquid suspension. The collection efficiency of the BioSampler at that flow rate is near 100% for particles above 1.5 μm (Kim et al. 2001).

The second module, for which in-depth details can be found in (Wang et al. 2016), starts with the transferring of the aqueous sample into a capped bottle for chemical reactions. In this step, concentrated acids (i.e., 4 M HCl for Fe and Mn, and 4 M HNO_3 combined with 1% H_2O_2 for Cr) are added to the sample at a volume ratio of 1:20 (acid:sample). The addition of acids results in very low pH levels (i.e., around 0.5) to ensure that nearly all metal species are solubilized during the 10 min residence time of this step. The pH is then adjusted to 5–7 for Fe-ferrozine and 7–8.5 for Mn-FAD reactions by adding sufficient amounts of 1 M NaOH. It should be noted that no NaOH is added for Cr measurements, since the Cr-DPC reaction is optimal at pH = 1. In the next step, oxidation/reduction agents (i.e., HA) are added to the sample solution to convert all different oxidation states of the target metals to a uniform state. In addition, for Mn measurements, the ethylenediaminetetraacetic acid (EDTA, 0.08 N) solution was added to the sample at a volume ratio of 1% to eliminate any possible interference from Fe existing in the ambient coarse PM sample (Majestic et al. 2007). For Cr, however, no oxidation agent was added to the sample solution, mainly because all the Cr(III) was already converted to Cr(VI) due to the addition of H_2O_2. After a total residence time of 10 min in the serpentine reactor and then in the reaction coil, the sample is transferred to a 10-cm path-length, optical flow cell (60 μL internal volume) MVFC (FIA-ZSMA-ML-100-TEF, Ocean Optics, Inc., Dunedin, FL, USA) for the spectrophotometry detection of the metals. The concentration of each metal was determined at the wavelength with the highest level of absorption for the corresponding analytical reagent (i.e., ferrozine at 562 nm for Fe, FAD at 450 nm for Mn, and DPC at 540 nm for Cr), while a wavelength of 700 nm, at which there is effectively zero absorptivity for the analytical reagents, was selected to determine the background sample absorption. It should be noted that the three target metals were not simultaneously measured, due mainly to limitations in the available equipment. Nonetheless, concurrent measurements can be easily implemented by splitting the concentrated slurry flow and using multiple spectrophotometry units in parallel. In addition, in this

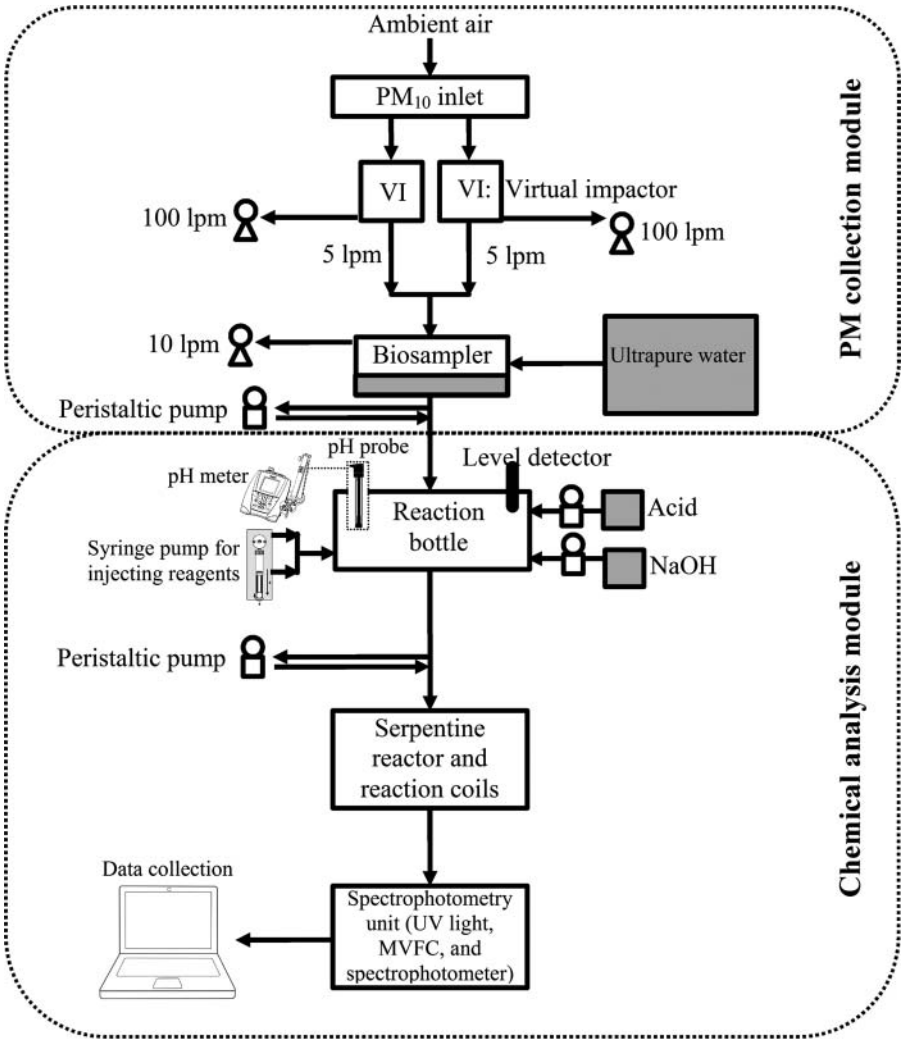

Figure 1. System schematic of the coarse PM metal monitor.

study we focused on measuring the total concentrations of the three metals, however, as indicated in our previous work by Wang et al. (2016), the system configuration can be easily modified to measure water-soluble and different oxidation states of the target metals. The former can be achieved by removing the acid digestion step and using inserting an in-line liquid filtration unit (e.g., a 0.20 μm polypropylene syringe filter) to remove the water-insoluble fraction before the spectrophotometric measurement. The latter can be achieved by performing measurements with and without the addition of the oxidation and reduction reagents. For instance, the water-soluble Fe can be measured by omitting the HCl addition in the measurement sequence and filtration before the sample passes through the MVFC. In addition, in order to measure Fe(II), the addition of the HA solution would be omitted from the procedure to prevent reducing Fe (III) to Fe(II). Furthermore, Fe(II) and total Fe can be measured using two distinct measurement lines, and the Fe(III) concentration can be easily calculated by subtracting Fe(II) concentration from that of total Fe. As illustrated by Wang et al. (2016), the same procedure can also be applied to Mn and Cr to measure water-soluble fraction and/or different oxidation states.

2.3. Field evaluation tests and continuous long-term operation

The developed system for the near-continuous measurement of Fe, Mn, and Cr in coarse PM was deployed at the Particle Instrumentation Unit (PIU), located on the University of Southern California's (USC) park campus, for field evaluation tests and continuous long-term run (i.e., approximately four months, from January to April 2016). As shown by previous studies performed at this location, this is a mixed urban site where ambient PM is largely impacted by vehicular emissions (Hasheminassab et al. 2014; Sowlat et al. 2016), as it is located 150 m downwind of a major freeway, i.e., I-110. It is also located approximately 3 km directly to the south of downtown

Los Angeles, CA, and less than 2 km to the southwest of another major freeway, i.e., the I-10.

Ambient coarse PM was collected in 2-h time intervals, resulting in 12 data points per day, and the concentrations of the target metals (i.e., Fe, Mn, and Cr) were subsequently measured using the system described above. After each day of sampling, the system was manually switched to measure the next metal species, therefore each metal was sampled every third day. Coarse PM sampling was done 6 days a week, starting on Tuesday and ending on the next Monday to incorporate weekend measurements as well. Every week, calibration and system maintenance was also performed on the day the system was stopped. Each metal was measured in 2 days per week. In addition, the sequence of measuring these metals was changed every week to make sure that we capture the variations of metals concentrations during the week as well as during the weekends.

In addition, 5 time-integrated 24-h filter samples were collected for each metal in parallel to the online measurements in order to compare the online concentrations to off-line measurements conducted on filters. For this purpose, another virtual impactor, with the same major and minor flow rates (i.e., 100 and 5 L/m, respectively) sampled in parallel with the on-line sampler. The air drawn by the minor flow of this virtual impactor was passed through 37-mm Teflon filters (Teflo, Pall Corp., Life Sciences, 1-μm pore, Ann Arbor, MI, USA), which were held in a 37 mm air sampling cassette (Zefon International Inc., Ocala, FL, USA). The filter samples were collected over a 24-h interval to ensure that sufficient coarse PM mass was collected for the subsequent elemental analysis using an magnetic sector inductively coupled plasma mass spectrometry (SF-ICPMS) instrument. To directly compare the 2-h online-measured data with those obtained from 24-h filter samples, the online data were averaged over 24 h.

Concurrent to the measurements of the target metals using the developed technique, ambient coarse PM mass concentrations were continuously measured using a coarse particle mass monitor previously developed, for which extensive details can be found in (Misra et al. 2001). Briefly, the continuous coarse particle mass monitor (CCPM) consists of three major components, including a PM_{10} inlet, a round nozzle VI with a 2.5-μm cut point, and a standard tapered element oscillating microbalance (TEOM 1400A, Thermo Fisher Scientific, MA, USA) instrument. In this system, particles are drawn through the VI with a total flow rate of 50 L/min. Coarse particles are then concentrated into the minor flow of 2 L/min and drawn through the TEOM for continuous measurement of PM mass concentrations, while $PM_{2.5}$ were drawn into the major flow (48 L/min).

2.4. SF-ICPMS analysis of filter samples

Following acid digestion of the PM, the total elemental composition of the particulate matter (PM) collected on the 37 mm Teflon filters was determined using magnetic sector inductively coupled plasma mass spectrometry (SF-ICPMS; Thermo–Finnigan Element 2) (Okuda et al. 2014). Filter membranes were placed in micro Teflon PFA digestion vessels and PM solubilized using a mixture of ultra-high-purity acids (1.0 mL of 16 M nitric acid, 0.25 mL of 12 M hydrochloric acid and 0.10 mL of hydrofluoric acid) in an automated microwave-aided digestion system (Milestone ETHOS+). This protocol effects a complete solubilization of all particle phases and element species. Digestates were diluted to 15 mL with high purity water (18 $M\Omega/cm^{-1}$) in pre-cleaned low-density polyethylene (LDPE) bottles and then analyzed by SF-ICPMS. Forty-nine elements were quantified. Propagated analytical uncertainties were estimated from the uncertainties (square root of the sum of squares method) of the SF-ICPMS instrumental analysis, method blanks, and digestion recoveries. The latter correspond to the standard deviation of replicate analyses of National Institute of Standards and Technology (NIST) Standard Reference Materials (SRM). Six solid samples of three SRMs were digested and analyzed with every analytical batch of samples. Further details of these protocols can be found in previous publications (Zhang et al. 2008; Saffari et al. 2013; Okuda et al. 2014).

3. Results and discussion

3.1. Calibration

For each metal, the measurement module (i.e., the spectrophotometry unit) of the developed system was calibrated using the dilution series prepared from the stock solution. Table 1 presents the results of the system calibration for each of the metals. As presented in the table, the calibration results indicated robust linear associations between metal concentrations and absorbance level at the respective analytical wavelength - the R-square of the calibration curve was above 0.99 for all of the metals. Regression line slopes of 0.0042 ($\pm$0.0002) (Abosorbance Unit (AU)/ppb), 0.0016 ($\pm$0.0001) (AU/ppb), and 0.0056 ($\pm$0.0004) (AU/ppb) for Fe, Mn, and Cr, respectively, confirm the high sensitivity of the long optical path spectrophotometric methods. It should be noted that system calibration was repeated multiple times during the sampling campaign as an additional quality assurance step to corroborate the validity of the on-line measurements. The limit of detection (LOD) for each metal was determined using the field method blanks prepared according to the following procedure: ultrapure

Table 1. Results of the system calibration for each of the individual metals measured.

Element	Range	Calibration curve (units of slope: AU[a]/ppb)	R^2	Limit of Detection[b] (LOD) (ppb)	Limit of Detection[c] (LOD) (ng/m^3)
Fe	0–200 ppb	$Y = 0.0042x - 0.0166$	0.99	0.3	0.25
Mn	0–100 ppb	$Y = 0.0016x + 0.0075$	0.99	0.2	0.17
Cr	0–100 ppb	$Y = 0.0056x - 0.0008$	0.99	0.2	0.17

[a]AU is absorbance unit.
[b]The LOD was calculated as three times the standard deviation of the field method blanks (i.e., ultrapure water as a blank sample plus the pertinent reagents).
[c]Estimated on the basis of a sampling flow rate of 200 L/min over a 2-h collection time.

water was first injected into the system and the relevant chemicals and reagents were added to the water as if this was an actual aerosol sample. Then, the blank sample was passed through the MVFC and the absorbance was measured. The LOD was estimated as three times the standard deviation of the field method blanks (Khlystov and Ma 2006; Majestic et al. 2007; Rastogi et al. 2009; Wang et al. 2016). According to the measurements and calculations mentioned above, the LODs were estimated to be 0.3 ppb (i.e., 0.25 ng/m^3), 0.2 ppb (i.e., 0.16 ng/m^3), and 0.2 ppb (i.e., 0.16 ng/m^3) for Fe, Mn, and Cr measurements (based on a flow rate of 200 L/min and a collection time of 2-h), respectively. Our system has also high measurement sensitivity, demonstrated by the signal-to-noise (S/N) ratios of 231, 83, and 38 for Fe, Mn, and Cr, respectively, based on the average metal concentration levels observed in the current study.

3.2. Comparison between online-measured data with filter samples data

As noted earlier, time-integrated 24-h filter samples were collected for each metal in parallel to the online measurements to verify the integrity of the readings by the developed sampler. Figure 2 presents the linear regression and correlation between the total (i.e., soluble plus insoluble) concentrations of the metallic species measured by the developed monitor and those obtained from ICP-MS analysis of the off-line filter samples collected in parallel. For these samples, the ranges of total concentrations were 30–180 ng/m^3 for Fe, 5–27 ng/m^3 for Mn, and 2–14 ng/m^3 for Cr. As shown in the figure, very good agreement was observed between the total concentrations of the metallic species measured by the developed monitor and those obtained from the ICP-MS analysis performed on the collected filters, based on the slope of

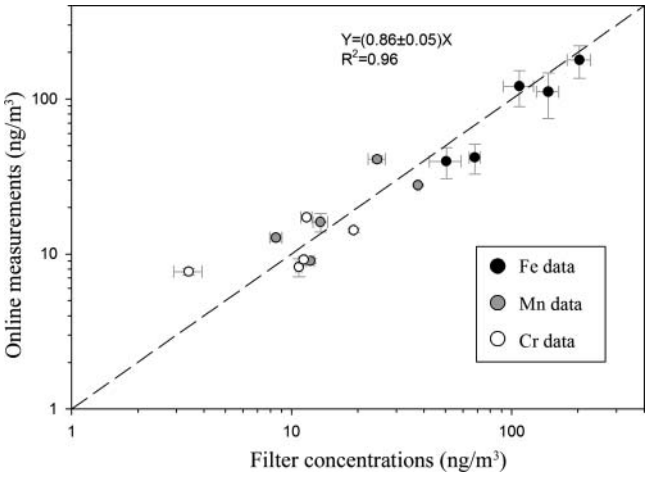

Figure 2. Linear regression and correlation between the metal concentrations measured online with off-line concurrent measurements obtained using filter samplers. Error bars represent one standard deviation of multiple online ($n = 12$) and offline ($n = 3$) measurements for each data point.

regression line (i.e., 0.86 ± 0.05) and the R-square value (i.e., 0.96). This agreement based on total concentrations indicates that the ambient coarse PM has been effectively digested. In addition, the average (±SD) online/filter concentration ratios were 0.83(±0.18), 0.93(±0.20), and 0.85(±0.11), respectively, for Fe, Mn, and Cr. The approximately 10% lower on-line versus off-line filter-based concentrations could be attributed to the loss of particles (mostly the insoluble fraction) on the walls and bottom of the Biosampler, particle loss in the tubing and in the reaction vessel, and the likely resistance of a small fraction of the insoluble part of PM-bound metals to the acid digestion/solubilization procedure.

Previous studies have indicated that these metal species in the coarse PM fraction are largely (between 60% and >90%) insoluble (Allen et al. 2001; Birmili et al. 2006; Wang et al. 2013; Shirmohammadi et al. 2015). Therefore, even though we did not directly measure the insoluble fraction of these metals, the very good agreement between the online-measured data and offline filter samples corroborates the method's capability to efficiently digest/solubilize the insoluble fraction and accurately measure the total concentration of Fe, Mn, and Cr.

3.3. Diurnal trends of Fe, Mn, and Cr in coarse PM concentrations and relationship to meteorological parameters in central Los Angeles

The developed monitor for online measurement of Fe, Mn, and Cr concentrations was deployed at the PIU site

for an approximate four month period, from January to April 2016, to assess the long-term performance of the system. Table 2 presents the summary statistics of the online-measured concentrations of coarse PM-bound Fe, Mn, and Cr during the study period. This table also provides the mass concentration of coarse PM measured using the CCPM running concurrently with the metal monitor at the PIU. As shown in the table, the average coarse PM mass concentration was 11.6 (±9.0) $\mu g/m^3$ over the study period. The coarse PM Fe concentrations averaged 57.8 (±43.0) ng/m^3 (ranging from 14.4–180.0 ng/m^3) and were higher than those of Mn (i.e., 15.0 (±10.3) ng/m^3, ranging from 2.2 to 37.2 ng/m^3) and Cr (i.e., 6.9(±4.1) ng/m^3, ranging from 1.5 to 17.2 ng/m^3). In addition, the levels observed in the present study are in concert with those previously reported in central LA at the same sampling site (i.e., the PIU), both for particle mass concentrations and coarse PM-bound metals (Cheung et al. 2011, 2012).

Data for meteorological parameters, including wind speed and direction, temperature, and relative humidity (RH) (Table 2) were acquired from the California Air Resources Board's (CARB) online database for the sampling site that is located in North Main St., downtown Los Angeles, which is located approximately 3 km northeast of our sampling site (i.e., the PIU). Figures 3a–c illustrates the average diurnal variation of meteorological parameters (i.e., temperature, wind speed, and RH) in the study area during our sampling campaign. As shown in the figure, maximum temperatures (around 20°C) were observed in the middle of the day, whereas RH (Figure 3b) peaked at night, reaching values up to 60%. The diurnal variations for wind speed (Figure 3c) exhibited a sharp peak (around 3 m/s) in the afternoon. These results are consistent with those reported previously in central Los Angeles (Cheung et al. 2011; Cheung et al. 2012).

Figure 4a presents the wind rose in the sampling site, indicating the direction and speed of the prevailing wind

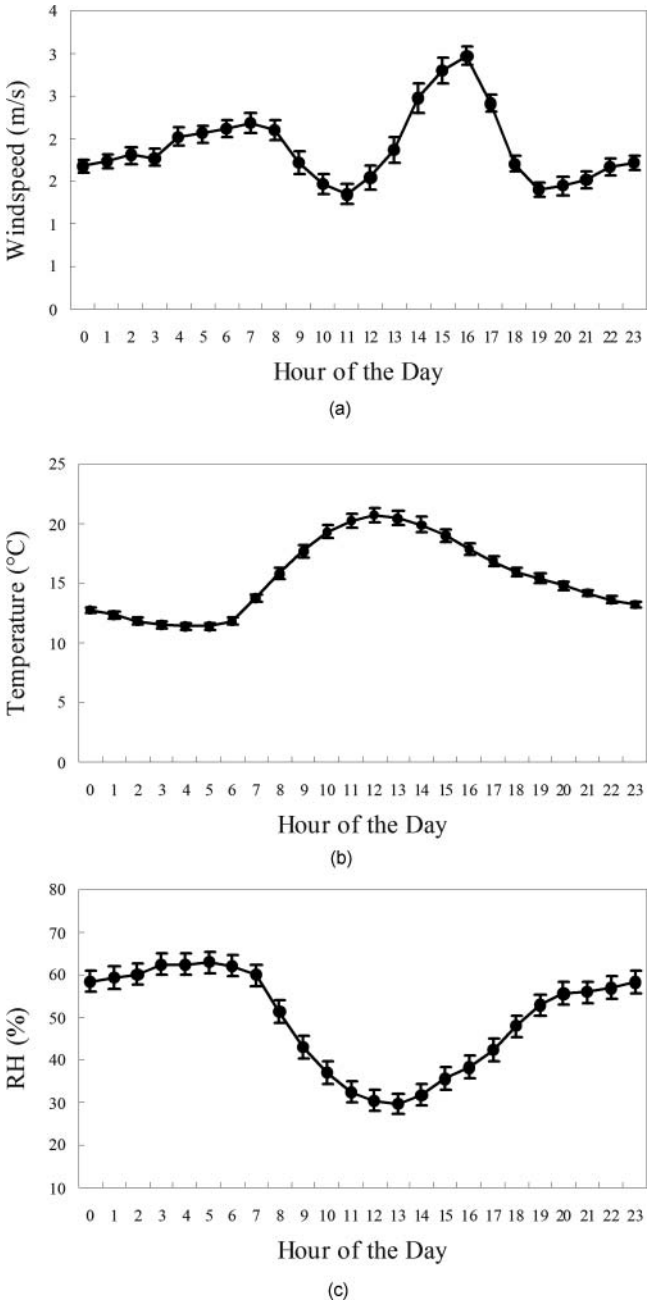

Figure 3. The diurnal variation of meteorological parameters in the study location averaged over the study period; (a) wind speed; (b) temperature; (c) relative humidity. Error bars represent one standard error (SE) of the mean.

Table 2. Summary statistics of the parameters collected over the entire study period.

Variables	Geometric Mean	Standard deviation	Minimum	Maximum
Fe (ng/m^3)	57.8	42.9	14.4	180.0
Mn (ng/m^3)	14.9	10.3	2.3	37.2
Cr (ng/m^3)	6.9	4.1	1.5	17.1
Wind speed (m/s)	1.9	1.2	0.9	8.5
Temperature (°C)	15.2	4.8	6.1	32.8
RH (%)	47.9	23.9	6.0	99.0
Coarse PM ($\mu g/m^3$)	11.6	8.9	1.20	55.1

in the study area during our campaign. As shown in the figure, the wind was most commonly blowing from the northeast (approximately 27% of the time), with the highest speeds ranging from 4 to 5 m/s. The second major wind direction during the sampling period was westerly and southwesterly winds, exhibiting even higher wind speeds (above 5 m/s).

Figures 4b–d present the concentrations of the metals in association with wind direction during the entire study period, presented separately for daytime

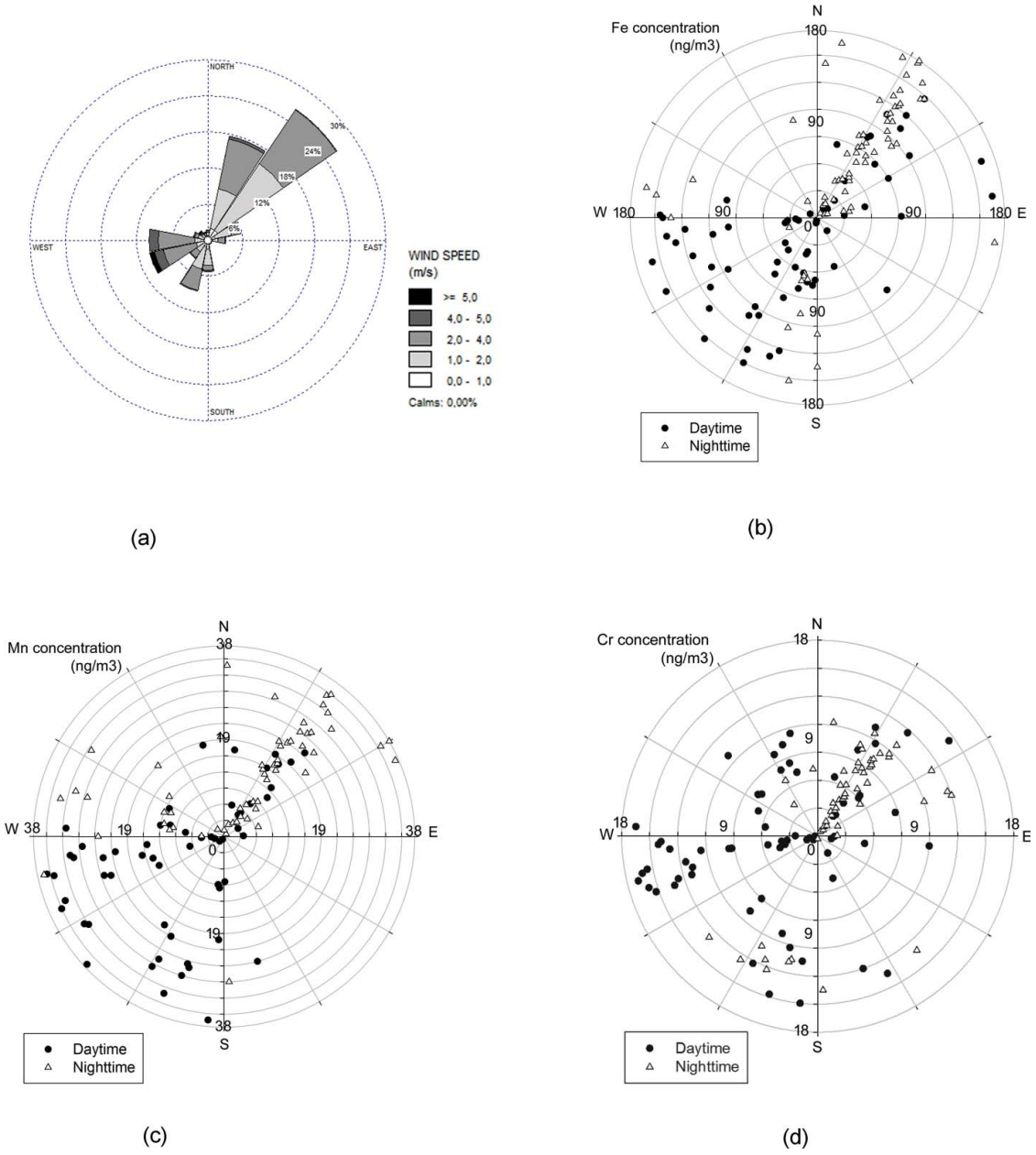

Figure 4. Prevailing wind direction and speed (a) during the study period and its relationship with concentrations of Fe (b), Mn (c), and Cr (d).

and nighttime. As can be seen from the plots, for Fe and Mn, the highest concentrations (i.e., 150–200 ng/m^3 for Fe and 30–40 ng/m^3 for Mn) were observed during two distinct periods, i.e., westerly/southwesterly winds during the daytime, and northeasterly winds during the nighttime. Our sampling site is located approximately 150 m to the east of the I-110 freeway; it is also in close proximity (less than 2 km to the southwest) to the I-10 freeway. Therefore, the observed high Fe and Mn concentrations during daytime westerly winds and nighttime northeasterly winds can be associated with traffic emissions (i.e., road dust/resuspension soil) brought to the site by prevailing winds from these two major freeways. It is also noteworthy that, for both Fe and Mn, although high concentrations were observed during nighttime northeasterly winds, the average daytime concentrations during westerly and southwesterly winds (i.e., 89.5 (±30.0) ng/m^3 and 19.4 (±11.6) ng/m^3 for Fe and Mn, respectively) were higher than those during nighttime (i.e., 64.5 (±39.9) ng/m^3 and 13.6 (±8.7) ng/m^3 for Fe and Mn, respectively). In contrast to the Fe and Mn trends, as can be observed in Figure 4d, the coarse PM Cr concentrations follow distinctly different trends that are suggestive of contributions of other potential local sources, including metal plating

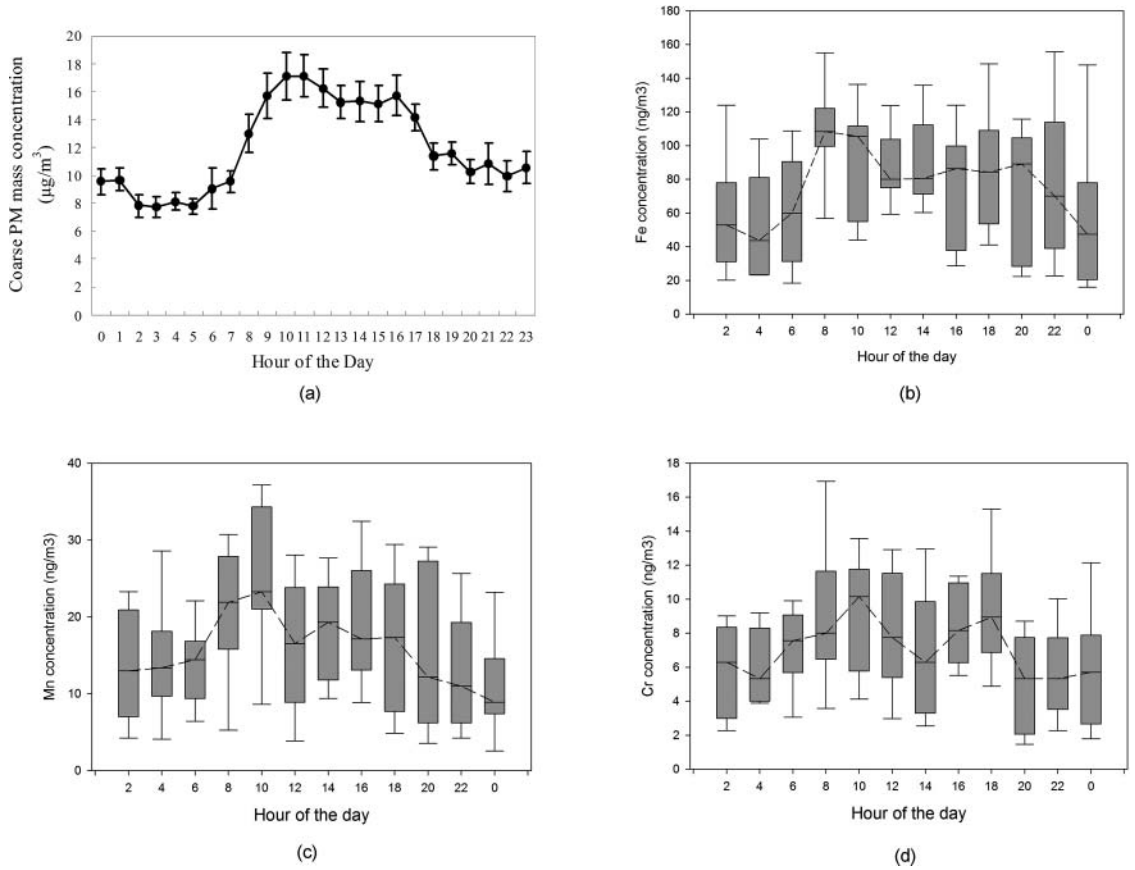

Figure 5. Diurnal variations of the coarse PM mass concentrations and the online-measured metal concentrations averaged over the study period; (a) coarse PM; (b) Fe; (c) Mn; (d) Cr. For panel a, the error bars represent one standard error (SE) of the mean. The box plots represent the interquartile range (the bottom and top lines of the box representing the first and the third quartiles, respectively). The line inside the box represents the median, while the whiskers above and below the box represent the 95th and 5th percentiles.

facilities using Cr-containing paints (Ospital et al. 2008; Propper et al. 2015), in addition to the road dust/resuspension soil noted earlier.

Figure 5a illustrates the diurnal variations of the coarse PM mass concentrations in the sampling location during the study period. As can be seen in the figure, the PM mass concentration starts to sharply increase at 8 am and reaches a maximum at 11-am-noon, decreasing to slightly lower ranges until 6 pm, and then sharply decreases down to the lowest values of 8–10 $\mu g/m^3$ at nighttime. This trend clearly indicates the impact of meteorological conditions and traffic volume on CPM mass variations. As shown in Figures 3a–c, during the midday period, we have the lowest RH and highest wind speed, both of which favor the resuspension of soil and road dust. This is also in agreement with the results from previous studies conducted in central LA at the same sampling site (Pakbin et al. 2010, 2011).

The average diurnal variations of Fe concentrations are shown in Figure 5b. The box represents the interquartile range (the bottom and top lines of the box representing the first and the third quartiles, respectively). The line inside the box represents the median, while the whiskers above and below the box represent 95th and 5th percentiles. As can be seen from the figure, two peaks were observed, one major peak during morning rush hours (8–10 AM) and one minor peak during late afternoon/early evening hours (4–8 PM), bringing the average Fe concentration up to around 90 ng/m^3, compared to the lower values of around 40 ng/m^3 during other hours of the day. These two peaks illustrate the impact of traffic-related emissions (most likely resuspended dust, given the size range of the PM being measured in this study) on CPM levels at the sampling site. This trend was also observed in Figure 4b, indicating high Fe concentrations during westerly and southwesterly winds, bringing atmospheric particles from the major freeway (i.e., I-110) located approximately 150 m to the west of our sampling site. There is also a smaller third peak in concentration observed in the middle of the day (1–3 PM), which corresponds to maximum temperatures and wind speeds and minimum RHs, as shown in Figures 3a–c. This peak can be attributed to southeasterly winds, which are most frequent in the middle of the day (Wang et al. 2015),

particularly in the cold season (Dec–March, as in this sampling campaign). This finding is also consistent with those reported by Sowlat et al. (2016), observing very high contributions from the soil/road dust during high temperatures and wind speeds and very low RHs.

Figure 5c shows the diurnal variations of Mn concentrations at the sampling location during the study period. As can be seen from the figure, the Mn concentrations peaked in the early morning (around 8–10 am), with an average concentration of 25 ng/m^3. As in the case of Fe concentrations, this peak can be attributed to the impact of traffic-related emissions (most likely resuspended dust) on CPM levels at the sampling site, which was also observed in Figure 3c, indicating the highest Mn concentrations during westerly and southwesterly winds, which carried road dust particles from the major freeway (i.e., I-110) to our sampling site. In contrast to the Fe diurnal variations, we did not observe a second peak in late afternoon/early evening hours; however, the Mn concentrations remained relatively high during the daytime hours (slightly less than 20 ng/m^3), which is the time period corresponding to maximum temperatures and wind speeds and minimum RHs, as shown in Figures 3a–c, indicating the probable influence of the soil dust factor. This finding is in concert with previous studies performed in central Los Angeles, showing the major influence of soil dust on coarse PM-bound Mn concentrations (Pakbin et al. 2010, 2011; Cheung et al. 2012; Shirmohammadi et al. 2015). Mn is therefore not dominated by mobile sources like Fe, and at least a major fraction of it in this size range probably originates from resuspension of soil dust. This is also confirmed by the results of the weekday/weekend analysis (Figure 7), which did not reveal any significant differences between Mn concentrations on weekdays compared to weekends.

Figure 5d indicates the diurnal variations of measured concentrations of Cr during the study period. Two distinct peaks were observed, one during morning rush hours (around 9 AM) and one during afternoon hours (3–5 PM), bringing the average Cr concentration up to around 12 ng/m^3, compared to the lower values of around 4–6 ng/m^3 during other hours of the day. Although these two peaks can be partly attributed to the impact of re-suspended road dust from 110 freeway, coarse PM-bound Cr may also be affected by other smaller local sources supported also by the association between Cr concentrations and wind direction data (Figure 4d). Figures 6a–c illustrate the diurnal variations of Fe, Mn, and Cr mass fractions averaged over the entire study period. As shown in the figures, the diurnal trends for the mass fractions were almost similar to those of

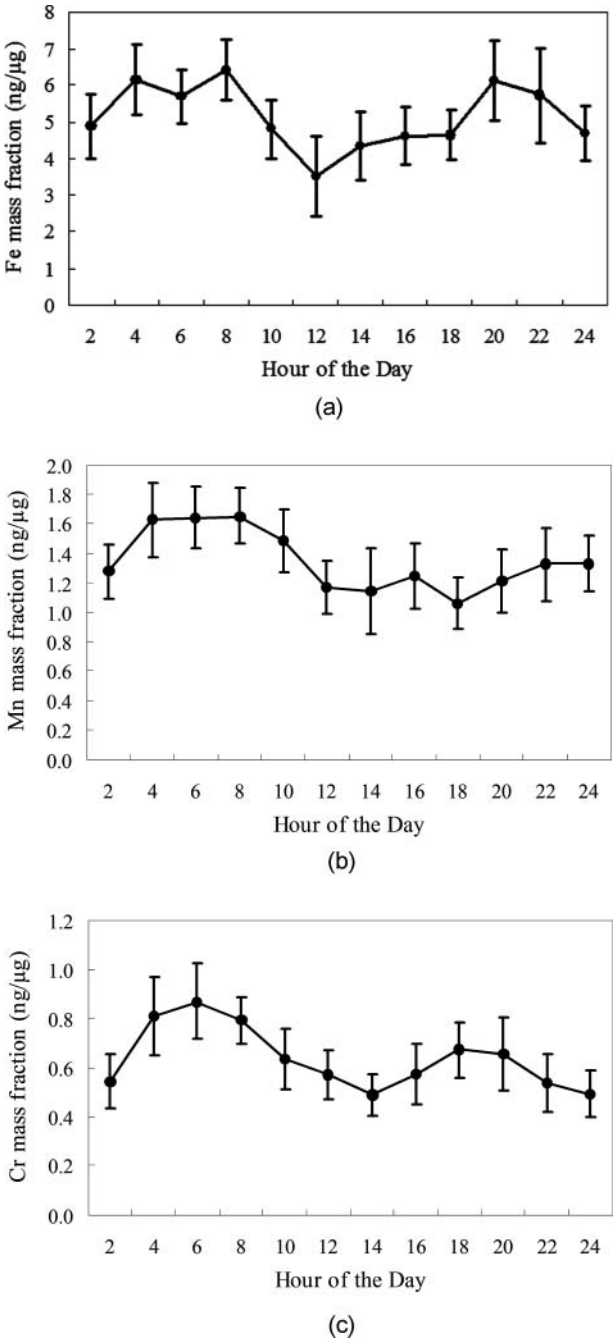

Figure 6. Diurnal variations of the mass fractions of the online-measured metal concentrations averaged over the study period; (a) Fe; (b) Mn; (c) Cr. Error bars represent one standard error (SE) of the mean.

airborne concentrations for all three of the metals, exhibiting major peaks in early morning for all the metals and a second peak in late afternoon/early evening hours for Fe. However, it is apparent from the diurnal trends of the mass fractions of these metals that the first peak occurs earlier in the morning (4–6 AM versus 8–10 AM), which is anti-correlated with coarse PM mass concentrations, implying the dilution of these metals by a less metal-enriched phase during morning rush hours.

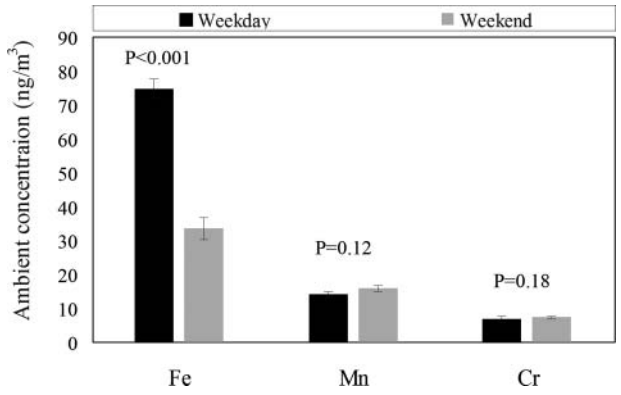

Figure 7. Weekday–weekend analysis of the metallic species concentrations during the study period. The P-values shown on the graph correspond to Mann–Whitney *U* test.

Figure 7 presents a weekday/weekend analysis for Fe, Mn, and Cr concentrations at the sampling site over the entire study period. As can be seen from the figure, the concentration of Fe was significantly higher during the weekdays (about 75 ng/m^3) compared to the weekends (around 33 ng/m^3) ($p < 0.001$), suggesting the major role of traffic in elevating Fe concentrations, which is consistent with the interpretation of the data in the metal rose plots as well as in the diurnal variation plots (Figures 5 and 6). However, the Mn and Cr concentrations were not statistically different ($p > 0.05$) between the weekdays and weekends (averaging about 15 ng/m^3 for Mn and about 7 ng/m^3 for Cr).

4. Summary and conclusions

In this study, a novel monitor was developed for near-continuous measurement of Fe, Mn, and Cr concentrations in ambient coarse PM (i.e., $PM_{10-2.5}$) with a time resolution of 2 hr. This monitor consisted of two modules, the first one utilizing two VIs connected to a modified BioSampler (i.e., liquid impinger) to draw and concentrate coarse PM into slurry samples, and the second one utilizing a Micro Volume Flow Cell (MVFC) coupled with spectrophotometry to measure metal concentrations. Our results indicate that all major species of the target metals can be efficiently digested by directly collecting ambient coarse PM into aqueous slurries. The validity of the online measurements was investigated using parallel time integrated filter-collected data obtained from ICP-MS analysis, which indicated very good agreement between the online measurements and parallel filters. The average concentrations of the three metals during the study period were 57.8 ng/m^3, 15.0 ng/m^3, and 6.9 ng/m^3 for Fe, Mn, and Cr, respectively, consistent with published data from the study site. Diurnal variations of these metals generally followed that of coarse PM mass concentrations, suggesting the influence of meteorological conditions and traffic sources on these metals in coarse PM. Results from the present study indicate that the developed monitor is capable of achieving measurements with high accuracy and reliability over long sampling periods with minimum supervision. These features, combined with the unique abilities of the system to measure water-soluble and different oxidation states of these metals make it a promising technology to achieve near-continuous measurements of metal concentrations in ambient coarse PM, enabling a better understanding of the atmospheric processes and sources involved in formation and transport of these redox-active metals in the coarse PM size range.

Funding

The authors would like to acknowledge the support of the USC Viterbi School of Engineering's Ph.D. fellowship award, as well as the Department of Chemistry, Sapienza University of Rome, for supporting in part Giulia Simonetti.

References

Argyropoulos, G., Besis, A., Voutsa, D., Samara, C., Sowlat, M. H., Hasheminassab, S., and Sioutas, C. (2016). Source Apportionment of the Redox Activity of Urban Quasi-Ultrafine Particles (PM 0.49) in Thessaloniki Following the Increased Biomass Burning due to the Economic Crisis in Greece. *Sci. Total Environ.*, 568:124–136.

Allen, A. G., Nemitz, E., Shi, J. P., Harrison, R. M., and Greenwood, J. C. (2001). Size Distributions of Trace Metals in Atmospheric Aerosols in the United Kingdom. *Atmos. Environ.*, 35:4581–4591.

Ayres, J. G., Borm, P., Cassee, F. R., Castranova, V., Donaldson, K., Ghio, A., Harrison, R. M., Hider, R., Kelly, F., and Kooter, I. M. (2008). Evaluating the Toxicity of Airborne Particulate Matter and Nanoparticles by Measuring Oxidative Stress Potential—a Workshop Report and Consensus Statement. *Inhal. Toxicol.*, 20:75–99.

Becker, S., Mundandhara, S., Devlin, R. B., and Madden, M. (2005). Regulation of Cytokine Production in Human Alveolar Macrophages and Airway Epithelial Cells in Response to Ambient Air Pollution Particles: Further Mechanistic Studies. *Toxicol. Appl. Pharmacol.*, 207:269–275.

Becker, S., and Soukup, J. (2003). Coarse (PM 2.5–10), Fine (PM 2.5), and Ultrafine Air Pollution Particles Induce/Increase Immune Costimulatory Receptors on Human Blood-Derived Monocytes but not on Alveolar Macrophages. *J. Toxicol. Environ. Health A.*, 66:847–859.

Birmili, W., Allen, A. G., Bary, F., and Harrison, R. M. (2006). Trace Metal Concentrations and Water Solubility in Size-Fractionated Atmospheric Particles and Influence of Road Traffic. *Environ. Sci. Technol.*, 40:1144–1153.

Brunekreef, B., and Forsberg, B. (2005). Epidemiological Evidence of Effects of Coarse Airborne Particles on Health. *Eur. Respir. J.*, 26:309–318.

Charrier, J. G., and Anastasio, C. (2012). On dithiothreitol (DTT) as a Measure of Oxidative Potential for Ambient Particles: Evidence for the Importance of Soluble Transition Metals. *Atmos. Chem. Phys. Discuss.*, 12:11317–11350.

Cheung, K., Daher, N., Shafer, M. M., Ning, Z., Schauer, J. J., and Sioutas, C. (2011). Diurnal Trends in Coarse Particulate Matter Composition in the Los Angeles Basin. *J. Environ. Monitor.*, 13:3277–3287.

Cheung, K., Shafer, M. M., Schauer, J. J., and Sioutas, C. (2012). Diurnal Trends in Oxidative Potential of Coarse Particulate Matter in the Los Angeles Basin and Their Relation to Sources and Chemical Composition. *Environ. Sci. Technol.*, 46:3779–3787.

Claiborn, C. S., Larson, T., and Sheppard, L. (2002). Testing the Metals Hypothesis in Spokane, Washington. *Environ. Health Perspect.*, 110:547.

Davis, D. A., Bortolato, M., Godar, S. C., Sander, T. K., Iwata, N., Pakbin, P., Shih, J. C., Berhane, K., McConnell, R., and Sioutas, C. (2013). Prenatal Exposure to Urban air Nanoparticles in Mice Causes Altered Neuronal Differentiation and Depression-Like Responses. *PLoS One*, 8:e64128.

Delfino, R. J., Sioutas, C., and Malik, S. (2005). Potential Role of Ultrafine Particles in Associations Between Airborne Particle Mass and Cardiovascular Health. *Environ. Health Perspect.*, 113:934–946.

Delfino, R. J., Tjoa, T., Gillen, D. L., Staimer, N., Polidori, A., Arhami, M., Jamner, L., Sioutas, C., and Longhurst, J. (2010). Traffic-related Air Pollution and Blood Pressure in Elderly Subjects With Coronary Artery Disease. *Epidemiology*, 21:10.

Dockery, D. W., and Stone, P. H. (2007). Cardiovascular Risks from Fine Particulate Air Pollution. *N. Engl. J. Med.*, 356:511–513.

Donaldson, K., Stone, V., Borm, P. J. A., Jimenez, L. A., Gilmour, P. S., Schins, R. P. F., Knaapen, A. M., Rahman, I., Faux, S. P., and Brown, D. M. (2003). Oxidative stress and Calcium Signaling in the Adverse Effects of Environmental Particles (PM 10). *Free Radic. Biol. Med.*, 34:1369–1382.

Fang, T., Verma, V., Bates, J. T., Abrams, J., Klein, M., Strickland, M. J., Sarnat, S. E., Chang, H. H., Mulholland, J. A., and Tolbert, P. E. (2015). Oxidative Potential of Ambient Water-Soluble PM 2.5 Measured by Dithiothreitol (DTT) and Ascorbic Acid (AA) Assays in the Southeastern United States: Contrasts in Sources and Health Associations. *Atmos. Chem. Phys. Discuss.*, 15:30609–30644.

Gauderman, W. J., Urman, R., Avol, E., Berhane, K., McConnell, R., Rappaport, E., Chang, R., Lurmann, F., and Gilliland, F. (2015). Association of Improved Air Quality with Lung Development in Children. *N. Engl. J. Med.*, 372:905–913.

Harrison, R. M., Jones, A. M., Gietl, J., Yin, J., and Green, D. C. (2012). Estimation of the Contributions of Brake Dust, Tire Wear, and Resuspension to Nonexhaust Traffic Particles Derived from Atmospheric Measurements. *Environ. Sci. Technol.*, 46:6523–6529.

Hasheminassab, S., Pakbin, P., Delfino, R. J., Schauer, J. J., and Sioutas, C. (2014). Diurnal and Seasonal Trends in the Apparent Density of Ambient Fine and Coarse Particles in Los Angeles. *Environ. Pollut.*, 187:1–9.

Hassanvand, M. S., Naddafi, K., Faridi, S., Nabizadeh, R., Sowlat, M. H., Momeniha, F., Gholampour, A., Arhami, M., Kashani, H., Zare, A., and Niazi, S. (2015). Characterization of PAHs and Metals In Indoor/Outdoor PM 10/PM 2.5/PM 1 in a Retirement Home and a School Dormitory. *Sci. Total Environ.*, 527:100–110.

Heal, M. R., Hibbs, L. R., Agius, R. M., and Beverland, I. J. (2005). Total and Water-Soluble Trace Metal Content of Urban Background PM 10, PM 2.5 and Black Smoke in Edinburgh, UK. *Atmos. Environ.*, 39:1417–1430.

Karlsson, A., Irgum, K., and Hansson, H.-C. (1997). Single-Stage Flowing Liquid Film Impactor for Continuous on-Line Particle Analysis. *J. Aerosol Sci.*, 28:1539–1551.

Khlystov, A., and Ma, Y. (2006). An On-Line Instrument for Mobile Measurements of the Spatial Variability of Hexavalent and Trivalent Chromium in Urban Air. *Atmos. Environ.*, 40:8088–8093.

Kidwell, C. B., and Ondov, J. M. (2001). Development and Evaluation of a Prototype System for Collecting Sub-Hourly Ambient Aerosol for Chemical Analysis. *Aerosol Sci. Technol.*, 35:596–601.

Kidwell, C.B., and OndovJ. M. (2004). Elemental Analysis of Sub-Hourly Ambient Aerosol Collections. *Aerosol Sci. Technol.*, 38:205–218.

Kim, S., Jaques, P. A., Chang, M., Froines, J. R., and Sioutas, C. (2001). Versatile Aerosol Concentration Enrichment System (VACES) for Simultaneous in Vivo and In vitro evaluation of Toxic Effects of Ultrafine, Fine and Coarse Ambient Particles Part I: Development and Laboratory Characterization. *J. Aerosol Sci.*, 32:1281–1297.

Li, N., Wang, M., Bramble, L. A., Schmitz, D. A., Schauer, J. J., Sioutas, C., Harkema, J. R., and Nel, A. E. (2009). The Adjuvant Effect of Ambient Particulate Matter is Closely Reflected by the Particulate Oxidant Potential. *Environ. Health Perspect.*, 117:1116–1123.

Majestic, B. J., Schauer, J. J., and Shafer, M. M. (2007). Development of a Manganese Speciation Method for Atmospheric Aerosols in Biologically and Environmentally Relevant Fluids. *Aerosol Sci. Technol.*, 41:925–933.

Majestic, B. J., Schauer, J. J., Shafer, M. M., Turner, J. R., Fine, P. M., Singh, M., and Sioutas, C. (2006). Development of a Wet-Chemical Method for the Speciation of Iron in Atmospheric Aerosols. *Environ. Sci. Technol.*, 40:2346–2351.

Miljevic, B., Fairfull-Smith, K. E., Bottle, S. E., and Ristovski, Z. D. (2010). The Application of Profluorescent Nitroxides to Detect Reactive Oxygen Species Derived from Combustion-Generated Particulate Matter: Cigarette Smoke—A Case Study. *Atmos. Environ.*, 44:2224–2230.

Misra, C., Geller, M. D., Shah, P., Sioutas, C., and Solomon, P. A. (2001). Development and Evaluation of a Continuous Coarse (PM10–PM25) Particle Monitor. *J. Air Waste Manage. Assoc.*, 51:1309–1317.

Moreno, T., Querol, X., Alastuey, A., Viana, M., Salvador, P., De la Campa, A. S., Artiñano, B., De la Rosa, J., and Gibbons, W. (2006). Variations in Atmospheric PM Trace Metal Content in Spanish Towns: Illustrating the Chemical Complexity of the Inorganic Urban Aerosol Cocktail. *Atmos. Environ.*, 40:6791–6803.

Ntziachristos, L., Froines, J. R., Cho, A. K., and Sioutas, C. (2007). Relationship Between Redox Activity and Chemical Speciation of Size-Fractionated Particulate Matter. *Particle Fibre Toxicol.*, 4:1.

Okuda, T., Schauer, J. J., and Shafer, M. M. (2014). Improved Methods for Elemental Analysis of Atmospheric Aerosols

for Evaluating Human Health Impacts of Aerosols in East Asia. *Atmos. Environ.*, 97:552–555.

Ospital, J., Cassmassi, J., and Chico, T. (2008). Multiple Air Toxics Exposure Study in the South Coast Air Basin. MATES III Draft Final Report, South Coast Air Quality Management District, Diamond Bar, CA, USA.

Pakbin, P., Hudda, N., Cheung, K. L., Moore, K. F., and Sioutas, C. (2010). Spatial and Temporal Variability of Coarse (PM10− 2.5) Particulate Matter Concentrations in the Los Angeles Area. *Aerosol Sci. Technol.*, 44:514–525.

Pakbin, P., Ning, Z., Shafer, M. M., Schauer, J. J., and Sioutas, C. (2011). Seasonal and Spatial Coarse Particle Elemental Concentrations in the Los Angeles Area. *Aerosol Sci. Technol.*, 45:949–963.

Perez, L., Tobias, A., Querol, X., Künzli, N., Pey, J., Alastuey, A., Viana, M., Valero, N., González-Cabré, M., and Sunyer, J. (2008). Coarse Particles from Saharan Dust and Daily Mortality. *Epidemiology*, 19:800–807.

Pérez, N., Pey, J., Querol, X., Alastuey, A., López, J. M., and Viana, M. (2008). Partitioning of Major and Trace Components in PM 10–PM 2.5–PM 1 at an Urban Site in Southern Europe. *Atmos. Environ.*, 42:1677–1691.

Peters, A., Veronesi, B., Calderón-Garcidueñas, L., Gehr, P., Chen, L. C., Geiser, M., Reed, W., Rothen-Rutishauser, B., Schürch, S., and Schulz, H. (2006). Translocation and Potential Neurological Effects of Fine and Ultrafine Particles a Critical Update. *Part. Fibre Toxicol.*, 3:1.

Pope, C. A., Burnett, R. T., Thurston, G. D., Thun, M. J., Calle, E. E., Krewski, D., and Godleski, J. J. (2004). Cardiovascular Mortality and Long-Term Exposure to Particulate Air Pollution Epidemiological Evidence of General Pathophysiological Pathways of Disease. *Circulation*, 109:71–77.

Pope, C. A., Burnett, R. T., Thun, M. J., Calle, E. E., Krewski, D., Ito, K., and Thurston, G. D. (2002). Lung Cancer, Cardiopulmonary Mortality, and Long-Term Exposure to Fine Particulate Air Pollution. *JAMA*, 287:1132–1141.

Propper, R., Wong, P., Bui, S., Austin, J., Vance, W., Alvarado, Á., Croes, B., and Luo, D. (2015). Ambient and Emission Trends of Toxic Air Contaminants in California. *Environ. Sci. Technol.*, 49:11329–11339.

Putaud, J. P., Van Dingenen, R., Alastuey, A., Bauer, H., Birmili, W., Cyrys, J., Flentje, H., Fuzzi, S., Gehrig, R., and Hansson, H.-C. (2010). A European Aerosol Phenomenology–3: Physical and Chemical Characteristics of Particulate Matter from 60 Rural, Urban, and Kerbside Sites Across Europe. *Atmos. Environ.*, 44:1308–1320.

Putaud, J.-P., Raes, F., Van Dingenen, R., Brüggemann, E., Facchini, M.C., Decesari, S., Fuzzi, S., Gehrig, R., Hüglin, C., and Laj, P. (2004). A European Aerosol Phenomenology—2: Chemical Characteristics of Particulate Matter at Kerbside, Urban, Rural and Background Sites in Europe. *Atmos. Environ.*, 38:2579–2595.

Rastogi, N., Oakes, M. M., Schauer, J. J., Shafer, M. M., Majestic, B. J., and Weber, R. J. (2009). New Technique for Online Measurement of Water-Soluble Fe (II) in Atmospheric Aerosols. *Environ. Sci. Technol.*, 43:2425–2430.

Saffari, A., Daher, N., Shafer, M. M., Schauer, J. J., and Sioutas, C. (2013). Seasonal and Spatial Variation of Trace Elements and Metals in the Quasi-Ultrafine (PM0.25) Particles in the Los Angeles Basin Metropolitan Area and Characterization of Their Sources. *Environ. Pollut.*, 181:14–23.

Shafer, M. M., Perkins, D. A., Antkiewicz, D. S., Stone, E. A., Quraishi, T. A., and Schauer, J. J. (2010). Reactive Oxygen Species Activity and Chemical Speciation of Size-Fractionated Atmospheric Particulate Matter from Lahore, Pakistan: An Important Role for Transition Metals. *J. Environ. Monitor.*, 12:704–715.

Shi, T., Schins, R. P. F., Knaapen, A. M., Kuhlbusch, T., Pitz, M., Heinrich, J., and Borm, P. J. A. (2003). Hydroxyl Radical Generation by Electron Paramagnetic Resonance as a New Method to Monitor Ambient Particulate Matter Composition. *J. Environ. Monitor.*, 5:550–556.

Shirmohammadi, F., Hasheminassab, S., Wang, D., Saffari, A., Schauer, J.J., Shafer, M.M., Delfino, R.J., and Sioutas, C. (2015). Oxidative Potential of Coarse Particulate Matter (PM 10–2.5) and its Relation to Water Solubility and Sources of Trace Elements and Metals in the Los Angeles Basin. *Environ. Sci. Process. Impacts*, 17:2110–2121.

Sowlat, M. H., Naddafi, K., Yunesian, M., Jackson, P. L., and Shahsavani, A. (2012). Source Apportionment of Total Suspended Particulates in an Arid Area in Southwestern Iran Using Positive Matrix Factorization. *Bull. Environ. Contam. Toxicol.*, 88:735–740.

Sowlat, M. H., Naddafi, K., Yunesian, M., Jackson, P. L., Lotfi, S., and Shahsavani, A. (2013). PM10 Source Apportionment in Ahvaz, Iran, Using Positive Matrix Factorization. *CLEAN Soil Air Water*, 41:1143–1151.

Sowlat, M. H., Hasheminassab, S., and Sioutas, C. (2016). Source Apportionment of Ambient Particle Number Concentrations in Central Los Angeles Using Positive Matrix Factorization (PMF). *Atmos. Chem. Phys.*, 16:4849–4866.

Tao, F., Gonzalez-Flecha, B., and Kobzik, L. (2003). Reactive Oxygen Species in Pulmonary Inflammation by Ambient Particulates. *Free Radic. Biol. Med.*, 35: 327–340.

Valavanidis, A., Fiotakis, K., Bakeas, E., and Vlahogianni, T. (2005). Electron Paramagnetic Resonance Study of the Generation of Reactive Oxygen Species Catalysed by Transition Metals and Quinoid Redox Cycling by Inhalable Ambient Particulate Matter. *Redox Rep.*, 10:37–51.

Verma, V., Polidori, A., Schauer, J. J., Shafer, M. M., Cassee, F. R., and Sioutas, C. (2009). Physicochemical and Toxicological Profiles of Particulate Matter in Los Angeles During the October 2007 Southern California Wildfires. *Environ. Sci. Technol.*, 43:954–960.

Viana, M., Kuhlbusch, T. A. J., Querol, X., Alastuey, A., Harrison, R. M., Hopke, P. K., Winiwarter, W., Vallius, M., Szidat, S., and Prévôt, A. S. H. (2008). Source Apportionment of Particulate Matter in Europe: A Review of Methods and Results. *J Aerosol Sci.*, 39:827–849.

Wang, D., Pakbin, P., Shafer, M. M., Antkiewicz, D., Schauer, J. J., and Sioutas, C. (2013). Macrophage Reactive Oxygen Species Activity of Water-Soluble and Water-Insoluble Fractions of Ambient Coarse, PM 2.5 and Ultrafine Particulate Matter (PM) in Los Angeles. *Atmos. Environ.*, 77:301–310.

Wang, D., Shafer, M. M., Schauer, J. J., and Sioutas, C. (2015). A New Technique for Online Measurement of Total and Water-Soluble Copper (Cu) in Coarse Particulate Matter (PM). *Environ. Pollut.*, 199:227–234.

Wang, D., Sowlat, M. H., Shafer, M. M., Schauer, J. J., and Sioutas, C. (2016). Development and Evaluation of a Novel Monitor for Online Measurement of Iron, Manganese, and Chromium in Ambient Particulate Matter (PM). *Sci. Total Environ.*, 565:123–131.

Weber, R. J., Orsini, D., Daun, Y., Lee, Y. N., Klotz, P. J., and Brechtel, F. (2001). A Particle-into-Liquid Collector for Rapid Measurement of Aerosol Bulk Chemical Composition. *Aerosol Sci. Technol.*, 35:718–727.

Zhang, Y., Schauer, J. J., Shafer, M. M., Hannigan, M. P., and Dutton, S. J. (2008). Source Apportionment of in-Vitro Reactive Oxygen Species Bioassay Activity from Atmospheric Particulate Matter. *Environ. Sci. Technol.*, 42:6502–7509.